Excluded Volume Effects on Polymer Chains Confined to Spherical Surfaces

Juan J. Cerdà,[†,‡] Tomás Sintes,[*,†] and Amitabha Chakrabarti[‡]

Departament de Fısica. Universitat de les Illes Balears, 07122 Palma de Mallorca, Spain, and Department of Physics, Kansas State University, Cardwell Hall, Manhattan, Kansas 66506-2601

Received May 21, 2004; Revised Manuscript Received November 25, 2004

ABSTRACT: We present results from extensive Monte Carlo simulations of flexible and semiflexible excluded-volume polymer chains confined to impenetrable spherical surfaces. Our results are compared with the theoretical predictions for ideal chains by Mondescu and Muthukumar (MM) (*Phys. Rev. E* **1998**, *57*, 4411) and Spakowitz and Wang (SW) (*Phys. Rev. Lett.* **2003**, *91*, 166102), respectively. The SW prediction is found to be in better agreement with our simulation results than the MM prediction in all the cases studied. Conformation of chains of length L and persistence length l_p restricted to move on a sphere of radius R can be reasonably described by the SW formalism in the regime $L/(2\pi) < R < 2l_p$. For $R/l_p > 2$, the mean square end-to-end distance, as a function of the chain length, evolves from a two-dimensional (2D) self-avoiding random walk behavior to a saturation value. A rigid rod behavior is recovered in the limit of short and stiff chains. Unlike ideal chains, excluded volume chains confined to a spherical surface of large enough radius display a transition from a disordered to an helicoidal state as chain stiffness is increased. We have characterized this transition through the bond orientational correlation function and the Monte Carlo results reflect a balance between the bending energy and the excluded volume interactions.

I. Introduction

Polymers restricted to move on a nonplanar surface are a subject of great interest in physics and biology for their exciting fundamental science as well as for their novel technological applications. Adsorption of polyelectrolytes onto colloidal particles[1] and micelles[2] leads to a restricted motion of the polymers on the surface in the limit of strong attractions. Such chain adsorption onto various nonplanar surfaces has been studied recently by several authors, both theoretically[3−7] and numerically.[8−13] Polymer adsorption is closely related to the problem of macroion complexation formation with polyelectrolytes. In particular, formalism used to study adsorption has recently been applied to the study of interesting DNA complexation with proteins like histones.[11]

Chain motion onto curved surfaces is also relevant to the problem of a polymer confined inside a cavity.[14,15] Due to entropic effects, flexible polymers tend to fill the available space with the highest concentration in the center of the cavity. Instead, very stiff chains tend to circle near the surface in order to minimize the bending energy. Therefore, rigid polymers behave as chains with an effective restricted motion close to the cavity surface. The problem of confined stiff chains turns out to be relevant for DNA packaging into virus capsids and vesicles and its release through nanopores.[16−20] Cryo-electron microscopy experiments for several viruses have shown that DNA molecules arrange within viral capsids in concentric circles involving an helical pitch.[21−23] For instance, Olson et al.[23] have observed that *T*4 bacteriophage genome forms a highly condensed series of concentric layers, spaced about 2.36 nm apart, that follow the general contour of the inner wall of the protein capsid.

Not only DNAs but also proteins also can be found encapsulated into nanometer sized vesicles.[24,25] Encapsulation of proteins in reverse micelles dissolved in low viscosity fluids is found to improve NMR protein studies by increasing the relaxation times.[26] Again, if a protein is highly confined, an effective restricted motion will take place.

Several recent theoretical work attempt to characterize properties of polymer chains enclosed in shells. Gaussian polymer chains on various types of surfaces in a D-dimensional space are studied by Mondescu and Muthukumar (MM).[27] For spherical surfaces, the averaged mean square end-to-end distance $\langle R_{ee}^2 \rangle$ for large polymer chains has been found to reach a constant value in this study, independent of the space dimensionality. On the other hand, for short chains, a linear dependence with persistence length and chain length has been predicted. Recently, Spakowitz and Wang (SW)[28] have developed a formalism to describe the statistical behavior of a semiflexible wormlike chain confined to a spherical surface and derived a closed expression for $\langle R_{ee}^2 \rangle$. Their model predicts different behaviors for the polymer chain depending on the relative size of the sphere and the chain persistence length.

While the predictions of MM and SW are strictly valid for ideal polymer chains, the present work focuses on confinement of more realistic polymer chains, interacting via excluded volume interactions, onto spherical surfaces. Our results are compared with previously mentioned theoretical predictions and serve as a check on the range of applicability of the ideal chain formalisms. In addition, our work provides insight into new chain conformations not described by the existing theories. To this end, we have performed extensive off-lattice Monte Carlo (MC) simulations for both flexible and semiflexible chains. For various degrees of rigidity of the chain, we have analyzed confined chain conformations as a function of the chain length and the radius

[†] Universitat de les Illes Balears.
[‡] Kansas State University.

10.1021/ma048989n CCC: $30.25
Published on Web 01/25/2005

of the sphere. We show that excluded volume chains behave similar to ideal chains and hence, reproduce most of the SW predictions when chains are smaller than the perimeter of the sphere and its degree of stiffness is large enough. For certain choices of the parameters, however, excluded volume chains show distinctly different behavior from ideal chains. For example, excluded volume chains undergo a disordered to helix transition within a particular range of parameters. This transition is totally absent in the ideal case.

The rest of the paper is organized as follows. In section II, we present a brief theoretical review summarizing the main features of the Mondescu−Muthukumar and Spakowitz−Wang theories. In section III, we describe the numerical model. In section IV, we present results of the Monte Carlo simulations and compare them with theoretical predictions. A characterization of the transition from the disordered to the helicoidal state is also presented in this section. Finally, we conclude in section V with a brief summary and discussion of the results.

II. Theoretical Review

A. The Mondescu—Muthukumar Theory. Brownian motion and polymer statistics on curved interfaces embedded in a D-dimensional space were studied in detail by Mondescu and Muthukumar.[27] Their work focused on the properties of polymer chains confined to spherical surfaces, cylinders, cones and torus of dimension $D - 1$. Polymers were assumed to behave as Gaussian chains containing N beads. By solving the diffusion equation for the probability distribution function, they derived an expression for the mean square end-to-end distance for a chain confined to a spherical surface:

$$\langle R_{ee}{}^2\rangle = 2R^2\left[1 - exp\left(-\frac{Ll}{2R^2}\right)\right]. \quad (1)$$

Here, R is the radius of the sphere, L is the chain length, and, l is the Kuhn length. This expression in independent of the dimensionality of the system. In the limit of $Ll \ll R^2$ the mean square end-to-end distance is approximately $\langle R_{ee}{}^2\rangle \approx Ll$, similar to an ideal random walk. On the other hand, for $Ll \gg R^2$, we get $\langle R_{ee}{}^2\rangle \approx 2R^2$. Small chains are expected to increase their mean square end-to-end distance linearly with their size and Kuhn length, whereas long chains are expected to reach a constant value closely related to the radius of the surface.

B. The Spakowitz—Wang Theory. In a more recent work, Spakowitz and Wang[28] introduced a novel representation of the differential geometry of an inextensible curve confined to a spherical surface and derived a precise description of the chain kinematics for a wormlike chain model. This formalism allows the evaluation of the mean square end-to-end distance in a closed form in a system where the interactions between chain segments are ignored.

In the SW theory, a chain of length L with a persistence length l_p, confined to a spherical surface of radius R has a mean square end-to-end distance given by

$$\langle R_{ee}{}^2\rangle = 2R^2\{1 - e^{-a}[\cosh(ab) + b^{-1}\sinh(ab)]\} \quad (2)$$

where

$$a = \frac{L}{4l_p} \text{ and } b = \left(1 - \frac{16l_p{}^2}{R^2}\right)^{1/2}$$

An oscillatory behavior is expected for $\langle R_{ee}{}^2\rangle$ for $R < 4l_p$, whereas for $R > 4l_p$, different scaling regimes are expected depending on relative values of the sphere radius, the persistence length, and, the chain length. Rigid rod scaling behavior is expected for chains with $L < 2l_p$, yielding $\langle R_{ee}{}^2\rangle \sim L^2$. On the other hand, ideal random walk behavior is found for polymer chains that verify $2l_p < L < R^2/(2l_p)$, yielding $\langle R_{ee}{}^2\rangle \sim Ll_p$. For large enough chains, $L > R^2/(2l_p)$, SW theory predicts an asymptotic behavior toward the uncorrelated end-to-end value, $\langle R_{ee}{}^2\rangle \approx 2R^2$.

Both Mondescu−Muthukumar and Spakowitz−Wang theories predict similar behaviors for large stiff chains. For small chains as well, both theories predict a linear growth of the mean square end-to-end distance with the persistence and chain lengths. For very short chains ($L \ll 2l_p$), however, SW predicts, in addition, a rigid rod regime.

III. Numerical Model

To check the range of validity of previous theories when excluded volume interactions are included in the model, we have performed extensive off-lattice three-dimensional Monte Carlo simulations. The polymer chain is represented by a pearl necklace model[29] containing N beads of diameter σ. We set $\sigma = 1$. The distance between consecutive beads along the chain is set to 1.1σ. Therefore, the chain length L is equal to $L = 1.1\sigma N$. Individual monomer moves consist of random wiggling motions at chain ends and rotations around the axis connecting the previous and following monomers for nonending monomers. Reptation-like motion for the whole polymer chain in a forward or a reverse direction is also allowed. Each move is accepted according to the standard Metropolis algorithm: $\exp(-\Delta U_{total}/\kappa_B T) > \eta$, where η is a uniform, random number between 0 and 1, and ΔU_{total} is the change in total energy of the system involved in the proposed motion. A link-cell method[30] has been implemented in the algorithm in order to improve computer efficiency.

In our model, U_{total} is given by

$$U_{total} = U_B + U_{ads} + \sum_{i=1}^{N}\sum_{i<j}^{N} V(r_{ij}) \quad (3)$$

Here, V is a hard sphere potential:

$$V(r_{ij}) = \begin{cases} 0 & \text{for } |r_i - r_j| > \sigma, \\ \infty & \text{for } |r_i - r_j| < \sigma \end{cases} \quad (4)$$

U_B is a bending energy term that accounts for the chain stiffness,

$$U_B = \sum_{\theta} \kappa(1 + \cos(\theta))^2 \quad (5)$$

θ being the bond angle between any two consecutive bonds and κ being the stiffness parameter. U_{ads} stands for an attractive interaction with the spherical surface

$$U_{ads} = n_{ads}\epsilon \quad (6)$$

where ϵ is the adsorption energy per monomer and n_{ads} is the number of adsorbed monomers onto the surface. We consider a monomer to be adsorbed when the center of the monomer lies within a distance $(R, R + \sigma)$ from the center of a sphere of radius R. To ensure a confinement i.e., a *total adsorption* of the chain on the spherical surface we need to consider a high adsorption energy. We have found that $\epsilon = -10\kappa_B T$ allows such a confinement.

The initial configuration of the self-avoiding polymer is randomly generated onto the surface of the sphere of radius R. One Monte Carlo step (MCS) is defined, as usual, as N trials to move the chain. The system has been equilibrated for 2×10^6 MCS. Subsequently, chain properties have been evaluated every 10 MCS and averaged over 10^5 measurements.

IV. Results and Discussion

A. Mean Square End-to-End Distance. To compare MM and SW predictions with the MC results for exclude volume chains, we have focused on the mean square end-to-end distance $\langle R_{ee}^2 \rangle$, as a function of the chain length L and stiffness parameter κ for several values of the sphere radius R.

To be consistent with the SW work, we first relate the persistence length l_p to a free polymer chain in 3D. The bond-angle correlation function[31] (BAC) has been used in order to calculate l_p. The BAC function is defined via the scalar product of two normalized bond vectors. The bond vector is defined as $\vec{b}_j = \vec{r}_{j+1} - \vec{r}_j$, $\vec{r}_k$ being the position of monomer k along the chain. Therefore

$$\mathrm{BAC}(i) = \left\langle \frac{\vec{b}_j \cdot \vec{b}_{j+i}}{|\vec{b}_j||\vec{b}_{j+i}|} \right\rangle = \langle \cos(\phi) \rangle \tag{7}$$

where $\phi(\vec{b}_j \vec{b}_{j+i})$ is the angle between the two bond vectors separated by i beads. $\langle ... \rangle$ indicates an average over all the polymer chain conformations. The BAC function decays exponentially with the distance between monomers, and the persistence length l_p is defined as the decay length of the BAC function,

$$\mathrm{BAC}(x) \sim \exp\left(\frac{-x\sigma}{l_p}\right) \tag{8}$$

We have computed the BAC function for free 3D polymer chains composed of N monomers and a stiffness parameter κ, and we have measured the persistence length $l_p(\kappa, N)$. These results are presented in Figure 1. We observe that the persistence length is independent of chain length, i.e., $l_p(\kappa, N) = l_p(\kappa)$ as expected. The limiting case of flexible chains corresponds to $\kappa = 0$. In this case, the persistence length is given by the bond length $l_p = 1.1\sigma$.

We have focused, first, on the behavior of flexible polymer chains. The mean square end-to-end distance $\langle R_{ee}^2 \rangle$ as a function of chain length L is studied for different sphere radius R. The results are shown in Figure 2. Note that for small enough L/R, $\langle R_{ee}^2 \rangle \sim L^{1.5}$. This exponent is nothing but twice the Flory exponent ($\nu = 3/4$) for a planar 2D self-avoiding random walk (SAW). The observed SAW breaks down for polymer chains that are long enough to feel the curvature of the sphere. This happens when the end-to-end distance becomes of the order of the sphere radius, then a maximum value for $\langle R_{ee}^2 \rangle$ is reached. Between, a transient linear regime is observed due to possible crossover

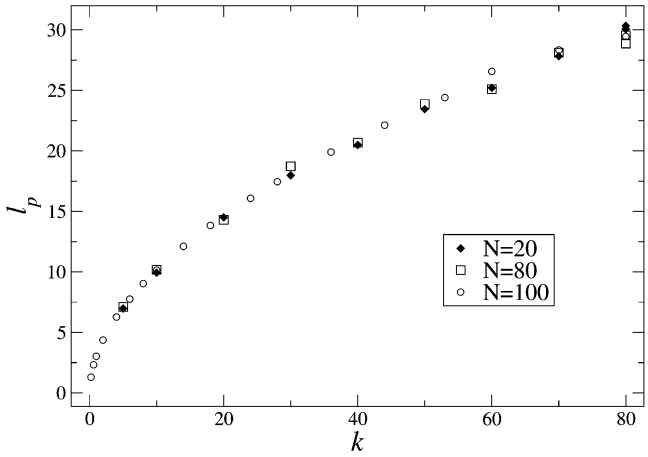

Figure 1. Persistence length l_p for a free 3-D polymer chain vs the stiffness parameter κ and the chain length L. The results indicate that the persistence length is independent of the chain length.

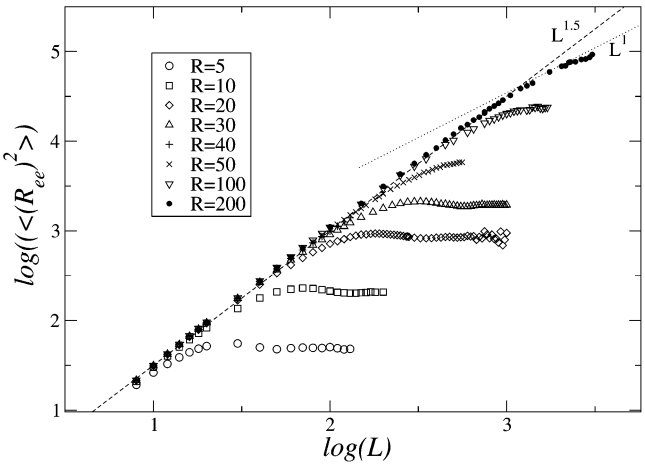

Figure 2. Log−log plot of the chain mean square end-to-end distance $\langle R_{ee}^2 \rangle$ as a function of chain length, L, for different values of the sphere radius R for flexible chains ($\kappa = 0$). Symbols depict our MC results. A dashed line of slope 1.5, and a dotted line of slope 1 are included to guide the eye.

effects. In comparison with the predictions of the SW formalism, a linear regime for chains with length satisfying $L < R^2/(2l_p)$ is found corresponding to our SAW regime but for ideal chains ($\nu = 1/2$). Once the maximum in $\langle R_{ee}^2 \rangle$ is reached, some amount of oscillations appear in the data before we enter the limit of uncorrelated chain ends where $\langle R_{ee}^2 \rangle = 2R^2$.

A comparison between the MC data for flexible polymer chains with the predictions of the MM and SW theories for small sphere radius ($R < 10$) is presented in Figure 3. We find MC results to be in better agreement with SW theory (solid lines) than with MM predictions(dashed lines).

For $R = 5$, due to a very small sphere radius, we reach the limit $l_p L \gg R^2$ even for very short chains, and $\langle R_{ee}^2 \rangle \approx 2R^2 = 50$ as predicted by SW and MM theories. An oscillatory behavior is observed in the MC data for all the radius studied for small L. However, the SW theory predicts such oscillations only for $R < 4l_p$. This upper limit is below the range of radius considered for flexible chains ($l_p = 1.1$), and thus, no oscillations can be expected. Finally, the SW and MM formalisms predict, in all of the cases studied, a mean square end-to-end distance smaller than MC results. The origin of this disagreement is in the excluded volume interactions

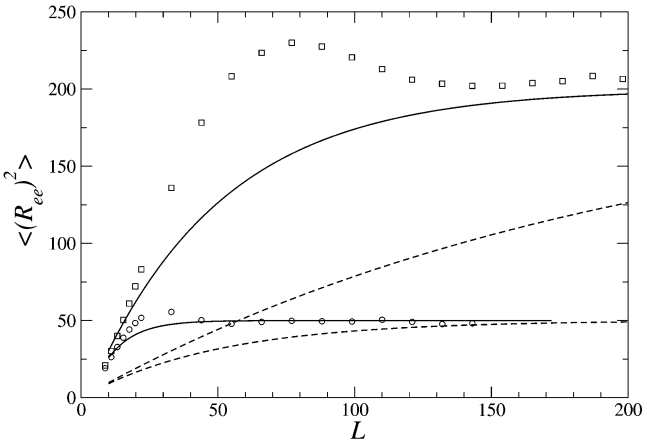

Figure 3. Mean square end-to-end distance $\langle R_{ee}^2 \rangle$ as a function of chain length L for $R = 5$ (○) and $R = 10$ (□). The persistence length is set to $l_p = 1$ ($\kappa = 0$). Solid and dashed lines correspond to the predictions of SW and MM, respectively.

between monomers which promote a stretching of the chain and cause an extra degree of orientational bond correlations.

To measure such orientational bond correlations we define the bond orientational correlation function BOC. Given two consecutive bond vectors $\vec{b}_i$ and $\vec{b}_{i+1}$, a unitary vector $\hat{p}_i$ perpendicular to the plane containing such vectors is defined as

$$\hat{p}_i = \frac{\vec{b}_i \times \vec{b}_{i+1}}{|\vec{b}_i \times \vec{b}_{i+1}|} \tag{9}$$

The BOC function is then defined as

$$\mathrm{BOC}(i) = \langle \hat{p}_j \cdot \hat{p}_{j+i} \rangle \tag{10}$$

$\langle ... \rangle$ being an average along the chain and over different polymer conformations. The BOC function becomes zero when bond vectors are uncorrelated. $\mathrm{BOC}(i) \rightarrow 1$ is expected when all the bonds follow the path of a maximum circle onto the sphere without changing the course. Negative values can be obtained for chains forming a hairpin structure where the bonds are anticorrelated.

In Figure 4, we plot the BOC function for short polymer chains ($N = 20$) confined to the surface of a sphere of radius $R = 10$ for several values of the stiffness parameter κ. A comparison between chains with excluded volume interactions (symbols) and ideal chains (lines) is presented. The degree of orientational correlation between bonds decreases as their distance in the chain sequence increases. The largest differences between short ideal and excluded volume chains are observed for flexible chains ($\kappa = 0$, $l_p = 1.1\sigma$). In such a case, the excluded volume effect causes an extra orientational correlation between monomers up to several positions in the chain sequence, whereas an ideal flexible chain loses its bond orientational correlation when bonds are separated more than two positions in the chain sequence. The excluded volume effect is particularly relevant in flexible chains since chain crossovers become banned. The chain monomers act as a steric barrier for other monomers forcing the chain to stretch out and $\langle R_{ee}^2 \rangle$ increases. For ideal chains crossovers take place easily and the monomer distribution is rather isotropic. As the stiffness of the chain increases, the BOC function for both ideal and excluded volume chains display a similar behavior (see Figure 4). It is worthwhile to mention that the stiffness contribution to the orientational bond correlations is larger than the excluded volume one for small polymer chains.

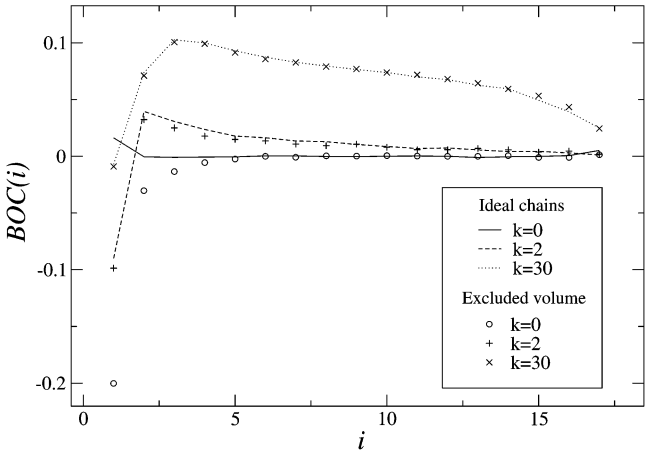

Figure 4. Bond orientational correlation function (BOC) vs the bond position for chains of length $N = 20$ confined to a sphere of radius $R = 10$. A comparison between ideal (lines) and excluded volume chains (symbols) is shown for several values of stiffness parameter $\kappa = 0$, 2, 30 (The corresponding persistence length is $l_p = 1$, 4.4, 18.1, respectively).

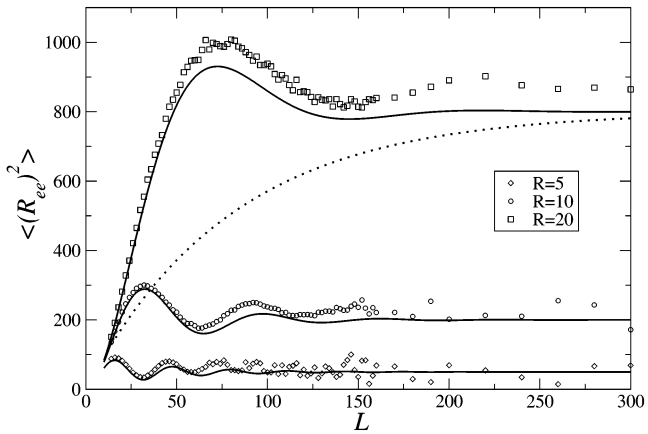

Figure 5. Mean square end-to-end distance $\langle R_{ee}^2 \rangle$ vs the chain length L, for stiff chains with persistence length $l_p = 10$ ($\kappa = 9.8$) and for small values of R/l_p ($R/l_p \leq 2$). Symbols are for our MC data, solid lines correspond to the SW predictions, and the dotted line stands for MM solution for a sphere of radius $R = 20$.

Above results indicate that for increasing value of the chain stiffness, a better agreement between SW theory and MC simulations should be observed. In Figure 5, we plot $\langle R_{ee}^2 \rangle$ vs the chain length L for stiff chains with a persistence length $l_p = 10$ in the regime $R \leq 2l_p$. We can observe a rather good agreement between the MC data (symbols) and the predictions of the SW theory (solid lines), specially for small L values. The position of the local maxima and minima of the oscillatory behavior can be explained in the following way. Local minima appear approximately when the chain length is a multiple of a full revolution around the sphere, that is, $L \approx 2n\pi R$. The conformation of a rather stiff polymer chain merely fluctuates from the one that is fully stretched and follows a maximum circle onto the sphere. On the other hand, the maxima are observed when $L \approx (2n + 1)\pi R$. In fact, chain fluctuations cause the

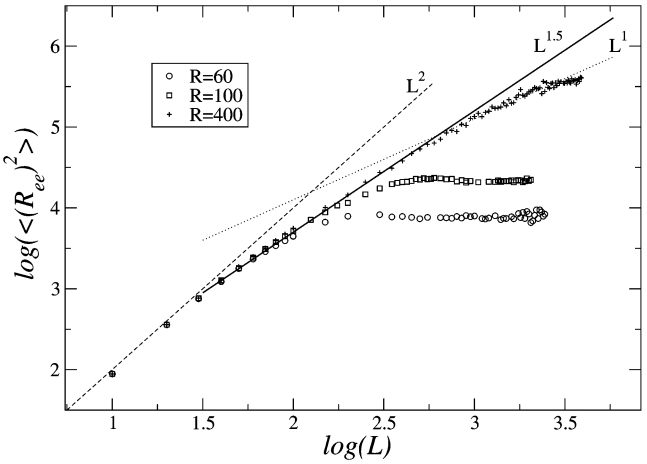

Figure 6. The log−log plot of the mean square chain end-to-end distance $\langle R_{ee}^2 \rangle$ vs the chain length L for high R/l_p ratios ranging from $R/l_p = 3$ to $R/l_p = 10$. The persistence length is set to $l_p = 20$. The dashed line of slope 2, the solid line of slope 1.5, and, the dotted line of slope 1 are guides to the eye.

maximum distance to be smaller than the diameter of the sphere $2R$ and the minimum distance to be larger than zero.

As L/l_p increases, the polymer structure can be rescaled to a flexible chain composed of blobs of size l_p. Thus, fluctuations around the conformation that occupies the maximum circle increases and the position of the chain ends become uncorrelated. At this stage $\langle R_{ee}^2 \rangle \rightarrow 2R^2$ for ideal chains. From Figure 5, we can observe that the presence of the excluded volume interactions leads to higher asymptotic values for $\langle R_{ee}^2 \rangle$ when compared to the ideal case. Furthermore, when the chain is large enough to complete a full revolution around a maximum circle onto the sphere, the excluded volume leads to an additional separation between successive revolutions. As a consequence, just after the first minimum, the differences between the SW predictions and the MC data are observed to increase.

The effect of increasing the surface radius is depicted in Figure 6. Polymer chains of size such that $L < 2l_p$ exhibit a rigid-rod behavior so that, in the limit of high R/l_p ratio, $\langle R_{ee}^2 \rangle \sim L^2$ (dashed line). The asymptotic value corresponds to a flat surface ($R \rightarrow \infty$). For $L > 2l_p$, the polymer behaves as a flexible chain when rescaled by l_p. In this case, and for large R values, we recover the characteristic 2D-SAW regime with $\langle R_{ee}^2 \rangle \sim L^{1.5}$ (solid line). This result is consistent with the previous simulations for flexible chains shown in Figure 2. By increasing the chain length, a transient regime, compatible with possible crossover effects, is observed (dotted line). Finally, a plateau is reached for $L > R^2/(2l_p)$. The size of the chain at which the end-to-end distance reaches its saturation value agrees with the limit predicted by the SW theory in the random walk regime.

For $R/l_p > 4$, the role of the excluded volume interactions is evident in the presence of a maximum in $\langle R_{ee}^2 \rangle$ and subsequent oscillations in it, as shown in Figure 7. Such behaviors of $\langle R_{ee}^2 \rangle$ are not predicted by either SW or MM theories. Nonetheless, the comparison shows that the SW results (solid lines) are in much better general agreement with the MC data than the MM predictions (dashed lines).

The behavior of $\langle R_{ee}^2 \rangle$ with the persistence length l_p has been examined for small and large sphere radius in Figure 8 and Figure 9, respectively. Our MC data

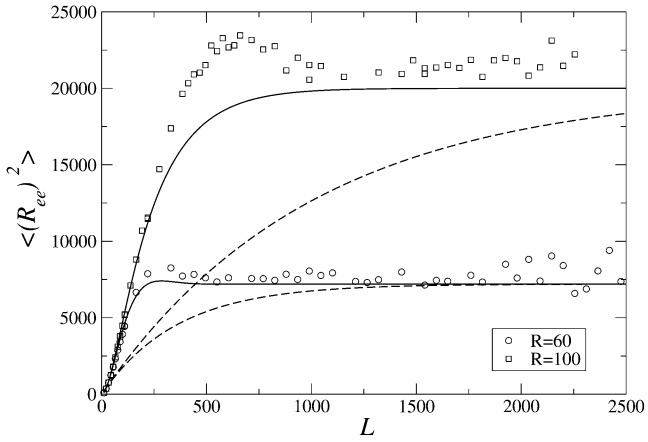

Figure 7. Mean square chain end-to-end distance $\langle R_{ee}^2 \rangle$ vs the chain length L for sphere radius $R = 60$ and $R = 100$. The persistence length is set to $l_p = 20$. Solid lines correspond to the SW predictions and dashed lines are MM results.

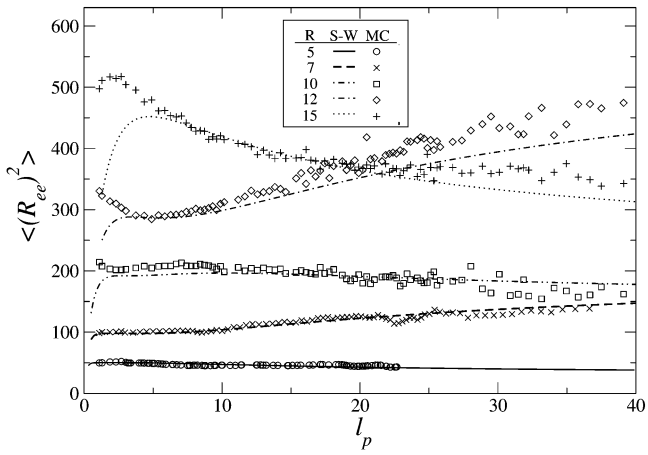

Figure 8. Mean square chain end-to-end distance $\langle R_{ee}^2 \rangle$ vs the persistence length l_p for small and intermediate radius of the sphere R. The chain length is set to $L = 110$. Symbols stand for our MC data and lines for the SW predictions.

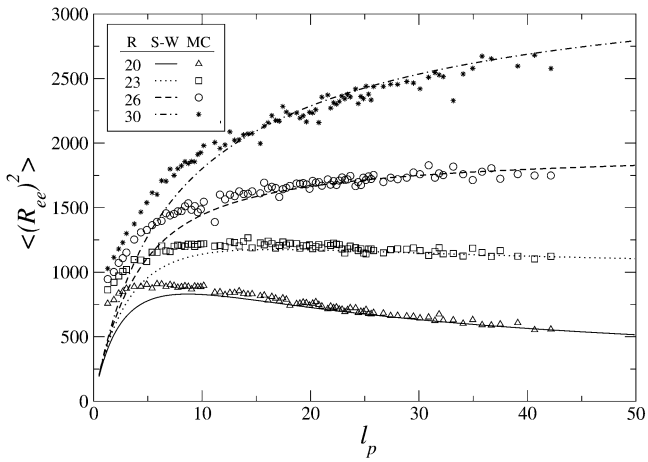

Figure 9. Same as Figure 8 for large sphere radius.

has been compared to the SW formalism for a polymer chain of length $L = 110$. Figure 8 shows increasing differences in l_p between the SW predictions and the MC results for various R between $R = 7$ and $R = 15$. These differences have their origin in the transition from disordered to helicoidal polymer conformations (studied in detail in the next section) as the chain stiffness is increased. Such transition is not observed

in ideal chains, and thus, are absent in the SW formalism. Nevertheless, SW formalism is still able to qualitatively reproduce the behavior of $\langle R_{ee}^2 \rangle$ with l_p which increases or decreases depending on the value of the sphere radius. It is interesting to mention that the MM formalism predicts a monotonic increase of the mean square end-to-end distance with the persistence length in all cases (see eq 1). This result does not agree with either SW theory and or with our MC data.

For large sphere radius (Figure 9), when the helicoidal state becomes impossible, a gradual recovery of the agreement between the SW predictions and the MC results is observed as l_p increases. In the limit of large l_p values, both SW and MC results match almost perfectly. This agreement is consistent with the fact that BOC functions of ideal and excluded volume chains are observed to be very similar for rigid chains confined to large spheres. Under such conditions, the behavior of an excluded volume chain will approach that of an ideal chain when the probability of contact among nonconsecutive monomers decreases and a similar chain stretching is expected in both cases. For $l_pL \ll R^2$ a linear dependence of $\langle R_{ee}^2 \rangle$ with l_p is observed, particularly for large R (see data for $R = 30$ in Figure 9). This linear regime agrees with the predictions of the SW and MM theories for $l_pL \ll R^2$.

At first sight, it may seem rather striking that by changing the radius of the sphere only slightly the mean square end-to-end distance changes its tendency to increase or decrease with l_p. This apparent paradox can be easily understood by taking into account the asymptotic value of $\langle R_{ee}^2 \rangle$ in the limit $l_p \to \infty$. When a polymer has a large degree of stiffness it tends to expand as much as possible and the most favorable energetic configuration is the one that occupies a maximum circle onto the sphere. Thus, the distance between chain ends depends on the ratio between the chain length L and the length of the maximum circle $2\pi R$.

The number of integer circles n_c covered by the polymer is

$$n_c = \mathrm{Int}\left(\frac{L}{2\pi R}\right)$$

and the arc length that joins the two chain ends is $l_{arc} = L - 2\pi R n_c$. It can be easily seen that the distance between such ends d_{ee}, is given by

$$d_{ee} = 2R \sin\left(\frac{l_{arc}}{2R}\right) \qquad (11)$$

In Figure 10, we plot the behavior of $\langle R_{ee}^2 \rangle$ with the radius of the sphere. We present a comparison between the data obtained in the MC simulations for several l_p value, and for a polymer chain of length $L = 110$, with the geometrical predictions (eq 11) derived for a chain that follows a maximum circle onto the sphere. We observe that the agreement improves when the chain stiffness is increased, as expected. An almost perfect match between the location of local maxima and minima are obtained. Any residual small differences, are due to the wiggling of the chain and the deviation from the large circle trajectory.

B. Transition from Disordered to Helicoidal Conformations. Although both ideal and excluded volume chains tend to occupy a maximum circle in the limit of $l_p \to \infty$, a fundamental difference between them arises due to the excluded volume interactions: chains

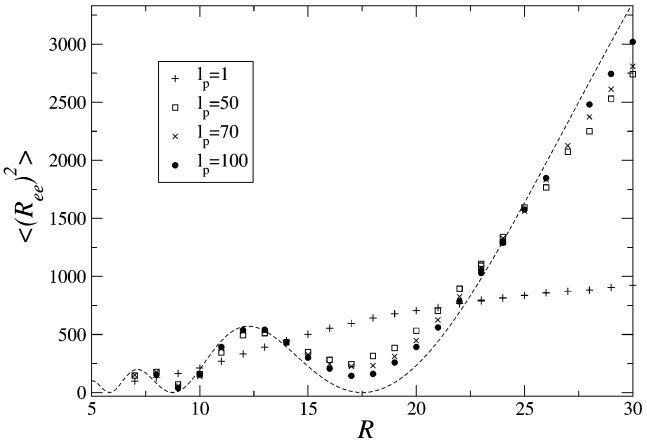

Figure 10. Mean square end-to-end distance $\langle R_{ee}^2 \rangle$ vs the sphere radius R, for several values of the persistence length. Chain length is set to $L = 110$. Symbols stand for our MC-data. The dashed line is the expected behavior from the geometrical calculations based on the maximum circle occupation by the chain (see eq 11).

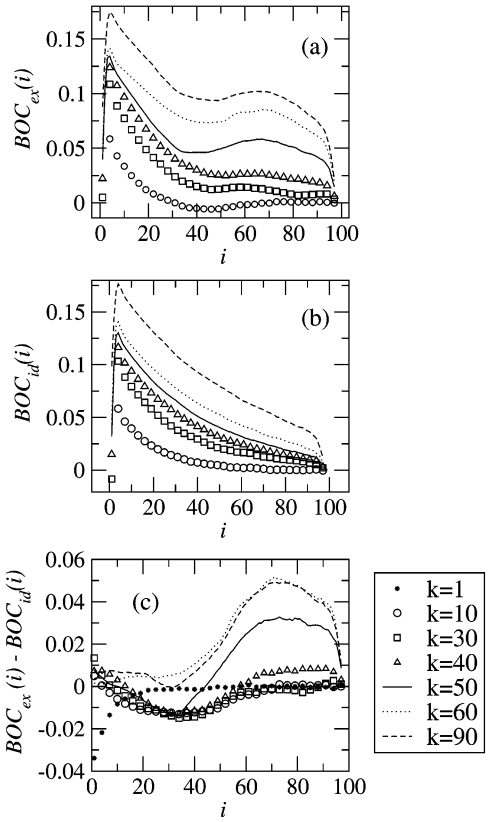

Figure 11. Bond orientational correlation function (BOC) as a function of bond position for chains of length $L = 110$ confined to a sphere of radius $R = 10$. (a) excluded volume chains; (b) ideal chains; (c) subtraction of part a from part b. The onset of the helicoidal state is reflected by the appearance of a local maximum at large values of bond position ($\kappa \geq 40$).

with exclude volume effects are observed to exhibit a transition from a disordered to an helicoidal conformation by increasing the chain stiffness, whereas no such transition to the helicoidal state has been observed for ideal chains. This different behavior between ideal and excluded volume chains as a function of chain stiffness can be probed by measuring the bond orientational correlation function (BOC) (see eq 10).

In parts a and b of Figure 11 we have plotted the BOC function for excluded volume and ideal chains, respec-

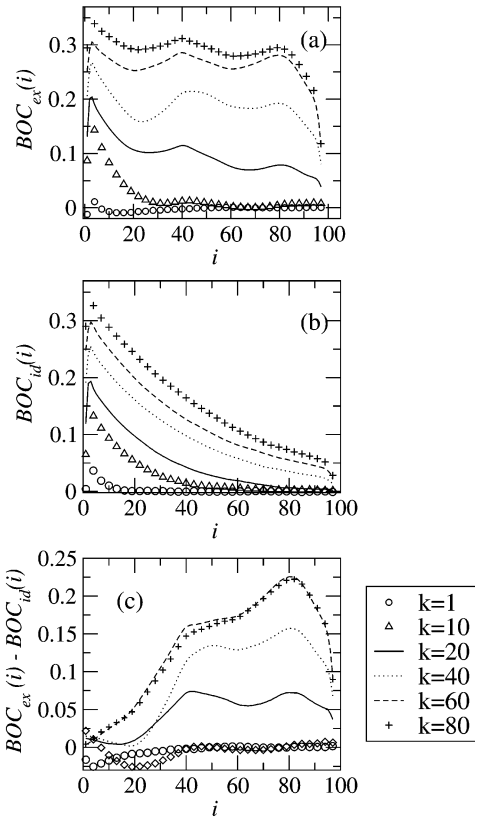

Figure 12. Same as Figure 11 for a polymer of length $L = 110$ confined to a sphere of radius $R = 7$.

tively. The polymer chain length has been selected to be $L = 110$, and it is confined to a sphere of radius $R = 10$. We can observe a rather different behavior between them as the stiffness parameter κ is increased. For ideal chains the BOC function decreases monotonically, independent of κ, whereas for excluded volume chains the BOC function displays a local maximum when the beads are separated in the chain by approximately $2\pi R/\sigma$ bond positions. The position of this local maximum is consistent with the fact that approximately $2\pi R/\sigma$ bonds are needed to complete a revolution around the sphere. Figure 11c shows the subtraction between the BOC function for excluded volume and ideal chains. The differences become evident for a stiffness parameter $k \geq 40$. It is precisely at this point where the transition from a disordered to an helicoidal state takes place. The results for a sphere of radius $R = 7$ are presented in Figure 12. The presence of a second maximum (see Figure 12c) at $i \approx 2\pi R/\sigma$ indicates that the polymer chain, following an helicoidal structure, has completed two revolutions around the sphere ($\kappa \geq 20$). It is worth to note that when the L/R ratio is increased the helicoidal state appears at smaller κ values. Typical conformations for $L = 110$ and $R = 7$ are shown in Figure 13. Figure 13a stands for an excluded volume chain with $\kappa = 2$, below the transition value. In Figure 13b we have plotted a typical conformation of an excluded volume chain with $\kappa = 50$, where a clear helicoidal structure can be seen. In Figure 13c a characteristic conformation of an ideal chain with identical rigidity ($\kappa = 50$) is plotted. Observe how, in the latter case, the helicoidal shape is lost and many chain crossovers take place. Such conformations have a smaller entropic penalty than the more ordered helicoidal conformations and, therefore, are preferred. We can conclude that excluded volume interactions are needed for the polymer chain to develop an helicoidal structure.

To characterize the transition to a helical state, one can try various ways of defining an order parameter.[11] Such effort was unsuccessful in our case where the chain is confined to the surface and did not allow us to probe the change from one configurational state to the other. In contrast, we have found the BOC correlation function (eq 10) to be an extremely useful tool. In fact, one can define an order parameter[9] by integrating the value of our bond correlation function BOC, and normalizing it by the number of monomers. However, it can be deduced from Figures 11 and 12 that this order parameter will increase for both ideal and exclude volume chains, and the difference between these two cases will be difficult to quantify. In contrast, the complete BOC correlation function contains details of the presence of strong correlations at large distances for exclude volume chains and this information allows us to show the presence of the transition. It also allows one to know whether the new helix state performs one or more revolutions around the sphere.

We should remark that $L > 2\pi R$ is needed to ensure that the chain will circle the sphere at least once. On the other hand, there is also a minimum value of R that makes it possible to accommodate a stable helix. Thus, there is an upper limit to the L/R ratio where helix structures can develop. By increasing L/R, we have seen the transition from disordered to helix structures to take place at smaller values of the stiffness parameter κ. For instance, for $L = 110$ the helix forms on a sphere of radius $R = 10$ at a critical stiffness parameter $\kappa_c = 40$,

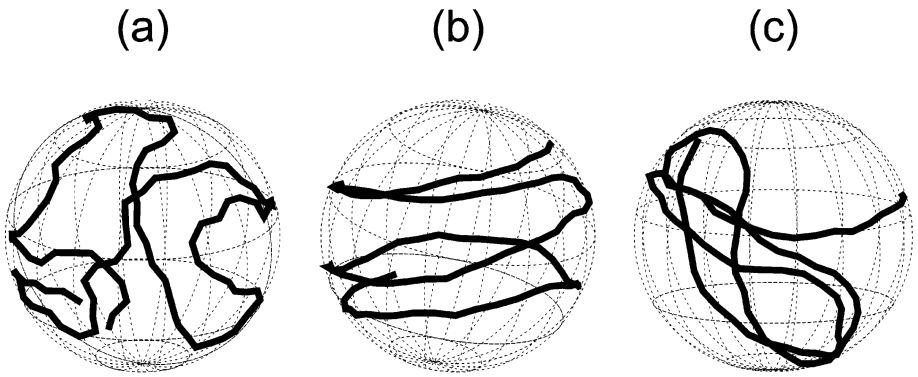

Figure 13. Snapshot of a typical conformation of a polymer chain of length $L = 110$ confined to a spherical surface of radius $R = 7$. Parts a and b correspond to excluded volume chains with a stiffness parameter: (a) $\kappa = 2$, below the transition point; (b) $\kappa = 50$ where the helix is formed. Part c stands for an ideal chain with the same stiffness as in part b. In contrast to the excluded volume chain, no helix structure is found.

for $R = 7$ at $\kappa_c = 20$ and for $R = 5.5$ at $\kappa_c = 5$. This fact can be easily understood in the following way. A small displacement of a monomer on the surface of the sphere induces a change in the $(1 + \cos(\theta))^2$ term of the bending energy U_B (see eq 5)that increases with decreasing the sphere radius. Thus, a smaller value of κ is needed to get the same ΔU_B.

The width of the surface potential that confines the chain to the surface is also expected to play a role in the helicoidal transition.[9] If the range of the attracting potential is large enough, a chain with excluded volume will be able to cross itself at different levels inside the adsorption layer. Eventually, this entails to a situation rather similar to what we observed for an ideal chain. In that case, the chain prefers a disordered conformation in which the entropic penalty is smaller than in an helicoidal state. We thus expect that the helicoidal transition to disappear if the width of the potential is large enough to allow the chain to self-cross at different levels. Note that entropically it is always favorable to have conformations that crosses itself rather than the helical conformation. And if the energetics also allow chain crossings, the helicoidal state must vanish at some point.

Next, we would like to comment on a work by Sakaue et al.,[9] who have studied the adsorption of a stiff chain onto a spherical core particle. A direct comparison with these results is not possible as the radius of the spherical surface is only 1.3 times the radius of the monomers in ref 9. In contrast, we have studied systems with a radius of at least 5 or more times the monomers radius. This is necessary in our case since we are considering a totally adsorbed or confined chain and a sphere of too small a radius cannot keep all the monomers of the chain trapped onto the surface. In fact, as we will see shortly, there is a lower limit of a critical radius for the existence of stable helical conformations for a given a chain length. In ref 9, a longer range potential is used which allows monomers to fly around without being confined onto the surface. This entails the possibility of having helicoidal conformations that do not affect all the chain. Helicoidal conformations under such conditions of small sphere radius and large width of potentials are not stable, and one must speak in terms of a probability for a chain to adopt an helicoidal conformation.

The transition point to the helix state can be qualitatively estimated if we consider a balance between the bending energy of a polymer chain,[32] which wants to wrap around the sphere along the large circle, and the excluded volume interaction, which depends on the density of segments, that prevents the chain segments to overlap. In Figure 14, we have plotted l_{pc} as a function of the radius of the sphere R for different chain lengths. In all the cases studied ($L \gg R$) we have found l_{pc} to grow roughly linearly with the radius of the sphere. This finding is consistent with the fact that the helicoidal structure is a simply manifestation of the excluded volume effects in the oscillatory regime in the SW theory. Thus, when a chain with excluded volume winds around a sphere, to make the end-to-end distance oscillatory, it must do it in a helical manner.

V. Concluding Remarks

We have characterized the behavior of excluded volume chains with restricted motion on spherical surfaces using off-lattice Monte Carlo simulations. A comparison with the Mondescu−Muthukumar and Spakowitz−Wang theories developed for nonexcluded volume chains has been presented.

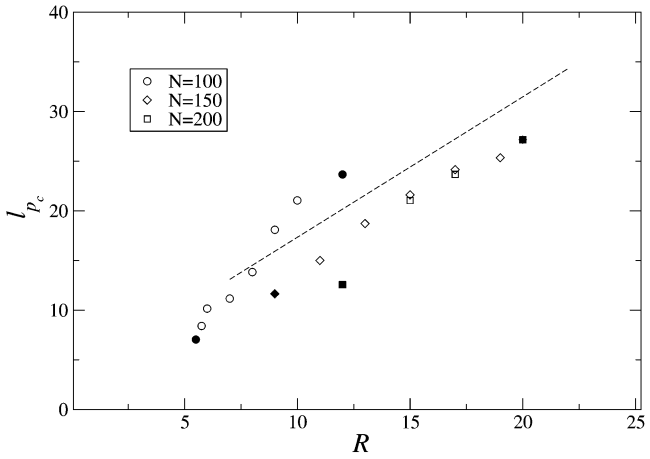

Figure 14. Characteristic persistence length l_{pc} for which the helix structure appears vs the radius of the sphere for several chain lengths. The upper bound and lower bound values of the radius where the helix forms are depicted by filled symbols. The dashed line is a guide to the eye and points out the linear relationship between l_{pc} and R when $L \gg R$.

We have found that the Spakowitz−Wang theory to be in better agreement with MC results than the Mondescu−Muthukumar formalism. However, we should bare in mind that the MM theory was not intended to account for the stiffness of the chain and deviation from our simulations are expected for large persistence length. This is true for the whole range of parameters studied. We have observed that our numerical data match almost quantitatively with the predictions of the SW formalism when (i) chain length is smaller than the length of the maximum sphere circumference and (ii) the chain is stiff enough, that is, the regime $L/(2\pi) < R < 2l_p$. Within this regime, the measurement of the bond orientational correlation function (BOC) for ideal and excluded volume chains provides very similar results. Thus, the behavior of excluded volume chains can be described, in this context, roughly as ideal chains, and the predictions of the SW formalism are reproduced.

The main difference between the SW theory and the MC results, for chains such that $L < 2\pi R$, is found in the measurement of the mean square end-to-end distance $\langle R_{ee}^2 \rangle$. The MC data is characterized by the presence of a maximum and subsequent relaxation oscillations toward the asymptotic value $2R^2$ for $R/l_p > 4$. The SW theory claims such oscillatory behavior to disappear for sphere radius larger than four times the persistence length, but excluded volume chains are observed to show such damped oscillations in all the cases we have examined.

MC data has shown that both, flexible and stiff excluded volume polymer chains exhibit, in a range of chain lengths, a self-avoiding random walk (SAW) behavior for $R/l_p > 2$ in contrast to the expected ideal random walk predicted by the SW formalism for $R/l_p > 4$. A rigid rod regime is found for $L < 2l_p$. For long polymers, beyond the SAW regime, $\langle R_{ee}^2 \rangle$ reaches a maximum plateau value for $L \geq R^2/(2l_p)$, in agreement with the predictions of the SW formalism.

One exciting feature observed in our MC simulations, is the transition from a disordered to helicoidal polymer conformation. This transition does not exist for ideal chains models and, thus, was not predicted by either

MM or SW formalisms. This transition has been studied in detail through the measurement of the BOC function. In the helicoidal state, long-range correlations are observed between bonds displaying local maxima at bond positions that complete a full revolution around the sphere. For a given a chain length, the transition is only found within a particular range of sphere radius. There is a lower bound of persistence length which provides the minimum rigidity required to stretch the chain along the spherical surface. This value decreases with the radius of the sphere. The relation between the characteristic persistence length and the radius of the sphere at the transition point is observed to be consistent with a balance between the bending energy due to deviations of the chain from the large circle trajectory and the excluded volume interactions. Similar behavior has been observed in the study of stiff polyelectrolyte adsorption on an oppositely charged spherical particles. In particular, the simulations carried out by Stoll and Chodanowski[10] show that by increasing the chain stiffness, solenoid conformations at the particle surface are progressively achived at small or zero values of the ion concentration. The latter corresponds to the case of strong polymer−surface interaction, in agreement with the assumption of polymer confinement implemented in our model.

Acknowledgment. J.J.C. and T.S. acknowledge financial support from the spanish MCyT grant no. BMF2001-0341-C02-01. The authors thank the reviewers for their useful comments.

References and Notes

(1) Sukhorukov, G. B.; Donath, E.; Davis, S.; Lichtenfeld, S.; Caruso, F.; Popov, V. I.; Möhwald, H. *Polym. Adv. Technol.* **1998**, *9*, 759.
(2) McQuigg, D. W.; Kaplan, J. I.; Dubin, P. L. *J. Phys. Chem.* **1992**, *96*, 1973.
(3) Birshtein, T. M.; Borisov, O. V. *Polymer* **1991**, *32*, 916. Birshtein, T. M.; Borisov, O. V. *Polymer* **1991**, *32*, 923.
(4) Schiessel, H.; Widom, J., Bruinsma, R. F.; Gelbart, W. M. *Phys. Rev. Lett.* **2001**, *86*, 4414.
(5) Netz, R. R.; Joanny, J.-F. *Macromolecules* **1999**, *32*, 9026.
(6) von Goeler, F.; Muthukumar, M. *J. Chem. Phys.* **1994**, *100*, 7796.
(7) Odijk, T. *Macromolecules* **1993**, *26*, 6897.
(8) Laguecir, A.; Stoll, S.; Kirton, G.; Dubin, P. L. *J. Phys. Chem. B* **2003**, *107*, 8056.
(9) Sakaue, T.; Yoshikawa, K.; Yoshimura, S.; Takeyasu, K. *Phys. Rev. Lett.* **2001**, *87*, 078105.
(10) Stoll, S.; Chodanowski, P. *Macromolecules* **2002**, *35*, 9556.
(11) Kunze, K.-K.; Netz, R. R. *Phys. Rev. Lett.* **2000**, *85*, 4389.
(12) Kong, C. Y.; Muthukumar, M. *J. Chem. Phys.* **1998**, *109*, 1522.
(13) Nguyen, T. T.; Shklovskii, B. I. *Physica A* **2001**, *293*, 324.
(14) Pais, A. C.; Miguel, M. G.; Linse, P.; Lindman, B. *J. Chem. Phys.* **2002**, *117*, 1385.
(15) Marenduzzo, D.; Micheletti, C. *J. Mol. Biol.* **2003**, *330*, 485.
(16) Purohit, P. K.; Kondev, J.; Phillips, R. *Proc. Natl. Acad. Sci. U.S.A.* **2003**, *100*, 3173.
(17) Muthukumar, M. *J. Chem. Phys.* **2003**, *118*, 5174.
(18) Arsuaga, J.; Tan, R. K.-Z.; Vazquez, M.; De Witt Sumners, Harvey, S. C. *Biophys. Chem.***2002**, 101−102, 475.
(19) Kindt, J.; Tzlil, S.; Ben-Shaul, A.; Gelbart, W. M. *Proc. Natl. Acad. Sci. U.S.A.* **2001**, *98*, 13671.
(20) Kiran Kumar, K.; Sebastian, K. L. *Phys. Rev. E* **2000**, *62*, 7536.
(21) Richards, K. E.; Williams, R. C.; Calendar, R. *J. Mol. Biol.* **1973**, *78* 255.
(22) Cerritelli, M. E.; Cheng, N.; Rosemberg, A. H.; McPherson, C. E.; Booy, F. P.; Steven, A. C. *Cell* **1997**, *91*, 271.
(23) Olson, N. H.; Gingery, M.; Eiserling, F. A.; Baker, T. S. *Virology* **2001**, *279*, 385.
(24) Colletier, J.-P.; Chaize, B.; Winterhalter, M.; Fournier, D. *BMC Biotechnol.* **2002**, *2*, 9.
(25) Zhou, H.-X.; Dill, K. A. *Biochemistry* **2001**, *40*, 11289.
(26) Wand, A. J.; Ehrhardt, M. R.; Flynn, P. F. *Proc. Nat. Academ. Sci.* **1998**, *95*, 15299.
(27) Mondescu, R. P.; Muthukumar, M. *Phys. Rev. E* **1998**, *57*, 4411.
(28) Spakowitz, A. J.; Wang, Z.-G *Phys. Rev. Lett.* **2003**, *91*, 166102.
(29) Baungärtner, A. In *Applications of the Monte Carlo Method in Statistical Physics*; Binder, K., Ed.; Topics in Current Physics 36; Springer-Verlag: Berlin, 1987.
(30) Allen, M.; Tildesley, D. In *Computer Simulation of Liquids.* Clarendon. Oxford, 1987.
(31) Micka, Uwe; Kremer, Kurt J. *Phys.: Condens. Matter* **1996**, *8*, 9463.
(32) Sakaue, T.; Löwen, H. *Phys. Rev. E*, **2004**, *70*, 021801.
(33) Grosberg, A.; Khokhlov, A. *Statistical Physics of Macromolecules*; American Institute of Physics: New York, 1994; page 84.

MA048989N